Low-Frequency Oscillations in Radiative–Convective Systems

QI HU* AND DAVID A. RANDALL

Department of Atmospheric Science, Colorado State University, Fort Collins, Colorado

(Manuscript received 10 March 1993, in final form 13 September 1993)

ABSTRACT

Although eastward propagation has long been considered one of the essential features of the Madden–Julian waves, recent observations have revealed a stationary or quasi-stationary component in the oscillations, particularly in measures of the diabatic heating rate. Wave–CISK theories of the low-frequency oscillations have struggled to explain the observed period and vertical structure of the waves. On the other hand, theoretical and numerical studies have shown that low-frequency waves strongly resembling the observed oscillations can be excited by specified low-frequency oscillations of the convective heating. A problem with the latter set of theories is that the cause of the oscillatory heating has not been satisfactorily explained. It is proposed here that the observed low-frequency wave motions are the response to forcing by an essentially stationary, self-excited oscillating heat source that is produced by nonlinear interactions among radiation, cumulus convection, and the surface fluxes of sensible heat and moisture. Feedback of the large-scale motions on the latent heating is not required. Results from two very different one-dimensional models are presented to support this hypothesis. The physical processes included in the models are essentially the same, that is, radiation, cumulus convection, and the surface fluxes of sensible heat and moisture; the first model is highly simplified, however, while the second includes relatively sophisticated parameterizations of all the relevant physical processes. Results from both models show low-frequency oscillations of the latent heating, temperature, and moisture. Experiments show that the oscillations are favored by a warm sea surface and weak surface wind speeds, consistent with the observed conditions over the Indian Ocean and the tropical western Pacific Ocean.

1. Introduction

The observed 30–60 day oscillation in the tropical atmosphere over the Indian and western Pacific Oceans involves many meteorological variables, including the zonal wind, surface pressure, temperature, and humidity (Madden and Julian 1971, 1972). Recent observations have revealed corresponding oscillations of various measures of cumulus activity (Murakami et al. 1986), including precipitation (Hartmann and Gross 1988) and outgoing longwave radiation (e.g., Weickmann and Khalsa 1990).

These low-frequency oscillations have been the subject of intense research because of their intraseasonal time scale, which suggests that intraseasonal climate anomalies may be predictable, and also because of their apparent relationships with the Indian summer monsoon (Yasunari 1979; Krishnamurti and Subrahmanyam 1982), the likelihood of tropical Pacific storms (Gray 1979), and the initiation of El Niño events (Lau and Chan 1985). Since tropical convection can force Rossby waves that propagate into the extratropics, the tropical 30–60 day oscillation can also influence the weather in middle latitudes (e.g., Rueda 1991).

Although the observed oscillation was described by Madden and Julian (1972) as an organized eastward moving transverse circulation oriented in the zonal plane with the upward branch in the region of intense convection, a growing body of observational evidence suggests that the convective heating associated with the oscillations has a stationary or quasi-stationary character. Yasunari (1979) showed that the observed oscillation of the cloudiness, averaged between 10°N and 15°N over the Indian and western Pacific Oceans, consists of an increase for a period of 20 to 30 days followed by a decrease over the next 10 days. These variations are geographically stationary, or nearly so. The localized character of the oscillation in cloudiness and convection is further documented in a study by Weickmann and Khalsa (1990). As shown in their Fig. 1, only the convection over the Indian and western Pacific Oceans oscillates; there are no oscillations of the convection east of the date line. In particular, there are no oscillations of convection over the Amazon Basin or the Congo Basin, even though a "Madden–Julian" signal is sometimes observed in the winds at those longitudes.

* Current affiliation: Atmospheric Science Research Center, State University of New York, Albany, New York.

Corresponding author address: Dr. David A. Randall, Department of Atmospheric Science, Colorado State University, Fort Collins, CO 80523.

As one might expect, the observed precipitation variations also appear to be essentially nonpropagating. Hartmann and Gross (1988) analyzed a 22-year time series of tropical precipitation and showed that the 30–60 day oscillation of precipitation occurs only at stations within or near the areas of intense convection in the Indian and western Pacific Oceans, for example, the SPCZ. They found that the oscillations of precipitation lead those of the zonal wind by 5–6 days. This phase difference suggests that the observed propagating low-frequency waves in the zonal winds are forced by the convection, rather than the reverse. Their results do not support the view that the oscillating component of the convective heating propagates spatially. Although there are some observational studies (e.g., Lau and Chan 1985; Knutson and Weickmann 1987) showing smoothed eastward propagation of heating-related fields, these are mostly based on composite and/or EOF methods, which are not well suited to studying propagation. At any rate, there is little observational evidence that the heating and the wave motions propagate together in a symbiotic fashion, as wave–CISK theories (discussed below) would suggest.

Hsu et al. (1990) reported a stationary, fluctuating, low-frequency latent heat source in the tropical western Pacific (see their Fig. 3). Waves appear to emanate from the region of the oscillating heat source and to propagate both eastward and poleward. The heating itself is relatively localized and does not appear to be symbiotically coupled with the propagating waves. Interestingly, Hsu et al. (1990) found that the eastward propagating 30–60 day waves typically complete only about a half-cycle before they dissipate. This appears to rule out the possibility that episodes of enhanced convection are triggered by the arrival, from the west, of eastward propagating waves that were forced by their predecessors. Recently, Zhu and Wang (1993) have attributed the "seesaw" of convection between the tropical Western Pacific and Indian Oceans to the interaction of convection with both eastward and westward propagating waves.

In summary, these observational studies show that an oscillating convective heat source over the warm Indian and western Pacific Oceans is strongly involved in the Madden–Julian oscillation. The observed eastward and poleward propagating 30–60 day waves appear to be consequences of the oscillating heat source. The wave motions propagate much more clearly than the heating itself, although there is some evidence that the heating travels with the waves over a relatively narrow range of longitudes.

These observations suggest that the interactions between the oscillatory heating and the wave motions are primarily, but not exclusively, in one direction; that is, the oscillatory heating drives the wave motions more effectively than the wave motions modulate the heating. Of course, it is a well-established fact that the large-scale motions in the tropics strongly affect the intensity and organization of cumulus convection. In particular, cumulus convection tends to be enhanced in regions of large-scale ascent. To the extent that propagating waves entail propagating regions of large-scale ascent, there will be a tendency for patches of enhanced cumulus heating to propagate with the waves. This is indisputable. What is more open to question, and what we wish to question in this paper, is whether the feedback of the waves on the heating is *essential* to the oscillating character of the heat source. We suggest that, on the contrary, such oscillations of the heating can arise in the absence of large-scale dynamical processes.

Theories of the Madden–Julian oscillation may be grouped into two categories:

(i) *wave–CISK theories* (e.g., Chang 1977; Lau and Peng 1987; Chang and Lim 1988; Wang 1988), and
(ii) *forcing-response theories* (e.g., Yamagata and Hayashi 1984; Hayashi and Miyahara 1987; Salby and Garcia 1987; Garcia and Salby 1987; Anderson and Stevens 1987).

The basic premise of wave–CISK theories is that the waves and the cumulus heating maintain each other and propagate eastward together via their mutual interactions and feedbacks. In order to maintain a continuous progression of waves at any given longitude, the waves have to complete a global circuit without dissipating. As discussed below, a basic problem with these theories is that they have difficulty explaining the observed phase speeds and vertical structures of the waves.

The wave–CISK theory (Hayashi 1970; Lindzen 1974) predicts a vertical wavelength of 8–9 km for waves with a Doppler-shifted phase speed of 10–15 m s^{-1} (consistent with a global circuit in 40–50 days). This vertical wavelength is less than half that of the observed 30–60 day waves in the tropics [15–30 km; see Madden and Julian (1972)]. In other words, a direct application of the classic wave–CISK theory predicts a phase speed twice as fast as observed, for waves of the observed depth.

Chang (1977) produced a new "viscous" mode by introducing a damping term that raised the order of the dispersion equation by one, and thereby produced a new "viscous" mode. Although the viscous mode's eastward phase speed is slow compared to the that of the classic wave–CISK modes, it has significant amplitude only near the heat source. Chang did not explain the mechanism that produces the oscillating heat source.

Along the same lines, Lau and Peng (1987) proposed a theory in which negative heating is not permitted. Although their results show modes that realistically combine deep vertical scales with slow phase speeds, these are a consequence of their *specified* heating profile which has a maximum near the 700-mb level (see their Table 2). Chang and Lim (1988) argued that

such a low-level heating maximum is necessary in order to generate slowly propagating modes.

Wang (1988) suggested that interactions between internal and external modes can generate slow, eastward propagating waves. Wang and Chen (1989) showed that the frictionally forced boundary-layer convergence of mass and moisture can induce such interactions. When frictional moisture convergence is strong enough, the growth of low-frequency planetary waves is favored. It remains to be seen whether this mechanism of Wang and Wang and Chen can explain how a low-frequency oscillation starts.

Neelin et al. (1987) and Emanuel (1987) hypothesized a surface evaporation–wind feedback to explain the Madden–Julian oscillation. In this theory, the heat source is maintained by both the waves through their interaction with the low-level flow on the east and the west sides of the heating. The maintenance and eastward propagation of convection in this theory depends on the existence of a mean easterly flow in the Indian and western Pacific Oceans. Such winds are not observed, however (e.g., Oort 1983).

We conclude that the wave–CISK theories have not been very successful in explaining the observed characteristics of the Madden–Julian oscillation.

The forcing-response theories are special cases of the general problem of waves forced by prescribed thermal forcing, as studied by Holton (1972) and Gill (1980). Holton showed that a specified oscillating tropospheric heat source excites waves in both the troposphere and the stratosphere; naturally, these waves have the same period as the heating. Their vertical scale is on the order of 20–30 km. For Kelvin waves, the zonal wavelength is linearly proportional to the vertical scale of the waves; deep modes have zonal wavenumber one.

Studies by Yamagata and Hayashi (1984), Hayashi and Miyahara (1987), Salby and Garcia (1987), and Garcia and Salby (1987), among others, provide examples of the application of this forcing-response concept to the Madden–Julian oscillation. Salby and Garcia showed that the response of the tropospheric winds to a stationary 30-day heating oscillation in the tropical western Pacific Ocean closely resembles that of the observed Madden–Julian oscillation. They found that the period of the oscillation increases with the period of the heating. They further demonstrated that eastward propagating waves excited in the lower troposphere are likely to succumb to dissipation even before reaching the Americas.

In summary, several studies have shown that slow eastward and poleward propagating waves with vertical wavelengths comparable to those of the Madden–Julian oscillation can be explained quite naturally as responses to localized, oscillatory tropical heating of low frequency. The key problem that has not been addressed in these studies is: What produces the localized oscillatory convective heat source?

In this paper, we propose a mechanism for self-excited, stationary, low-frequency oscillations of tropical cumulus convection. We present evidence that such low-frequency convective oscillations can result from interactions among radiation, cumulus convection, and the surface moisture flux. As shown in Fig. 1, the most important difference between our hypothesis and the wave–CISK theories of the intraseasonal oscillation is that our theory does not require any feedback of the waves on the convection in order to maintain the oscillations. We use two numerical models, with vastly different physical parameterizations, to provide support for this hypothesis. In order to focus on the localized oscillation, these models are one-dimensional; large-scale dynamics is deliberately eliminated.

In section 2, a "quick-look" model is presented. Results from this model show a 30–60 day oscillation of the precipitation rate and other fields. The mechanism responsible for the oscillations is discussed. In section 3, a one-dimensional model derived from the CSU GCM is applied to the same problem. Section 4 gives a summary.

2. A "quick look" model

a. Formulation

Model 1 is designed to be extremely simple, and as a result it is also extremely crude. It consists of a one-dimensional, active atmosphere above a passive ocean. The sea surface temperature (SST) is fixed, as is the surface wind speed, which must be treated as an external parameter because of the neglect of large-scale dynamics. Seventeen layers, of equal pressure thickness, are provided between 1000 and 200 mb.

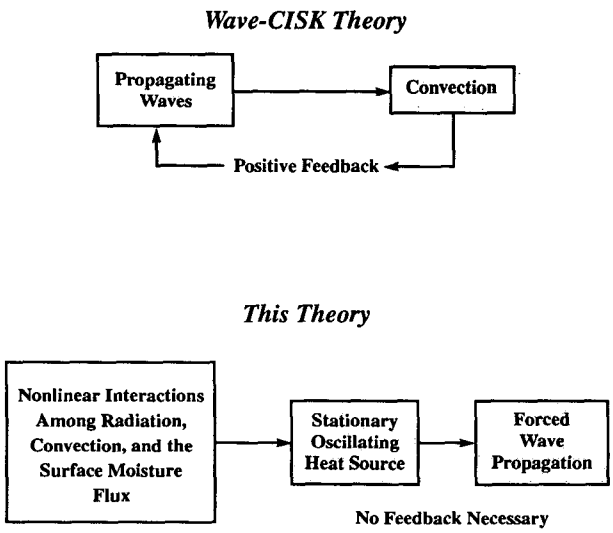

FIG. 1. A schematic diagram contrasting our theory with the wave–CISK theory.

Moist convection and large-scale saturation are included as in the moist convective adjustment of Manabe et al. (1965). The surface fluxes are parameterized using the bulk aerodynamic formulas, using the prescribed constant wind speed and a constant surface transfer coefficient. The effects of the surface fluxes of sensible heat and moisture are assumed to decrease exponentially with height, with an e-folding depth of about 1 km. No cloud–radiation interactions are included. The effects of solar radiation are also neglected. The effects of longwave radiation are parameterized by "Newtonian cooling"; that is,

$$\frac{Q_R}{c_p} = \frac{T_E(p) - T(p)}{\tau}.$$

Here Q_R/c_p is the radiative cooling rate, $T_E(p)$ is the pure radiative equilibrium temperature profile, and τ is the radiative relaxation time. Unless otherwise stated, we use $\tau = 20$ days and specify $T_E(p)$ following Manabe and Möller (1961). The model is integrated with a simple forward time-stepping scheme.

b. Results

1) CONTROL RUN

Using the parameter values given in Table 1, we integrated model 1 for 2000 days, starting from an arbitrary initial condition. The time step used was 30 minutes.

Figure 2a shows the precipitation rate as simulated during the first 500 days. After an adjustment period of about 120 days, very regular oscillations are apparent. Fourier analysis (Fig. 2b) shows that major period is about 34 days. Although the precipitation rate fluctuates, it never goes to zero; convection is always active.

Figures 3a–c show, respectively, the variations of perturbation temperature (T'), mixing ratio (q'), and radiative cooling rate (Q_R'), during the 100-day period

TABLE 1. Standard values of parameters in model 1.

Parameter	Value	Definition
C_D	1.5×10^{-3}	Drag coefficient
C_p	1.004×10^3 J K^{-1} kg^{-1}	Heat capacity at constant pressure
L	2.5×10^6 J kg^{-1}	Latent heat of condensation
g	9.806 m s^{-1}	Gravitational acceleration
ρ_0	1.10 kg m^{-3}	Density of air at the surface level
H	1000 m	Scale height of moisture
p_s	1000 mb	Pressure at the surface
p_T	200 mb	Pressure at model top level
$\hat{p}$	650 mb	Pressure level at which the turbulent mixing vanishes
T_0	300 K	Reference temperature
Θ_0	303 K	Reference potential temperature

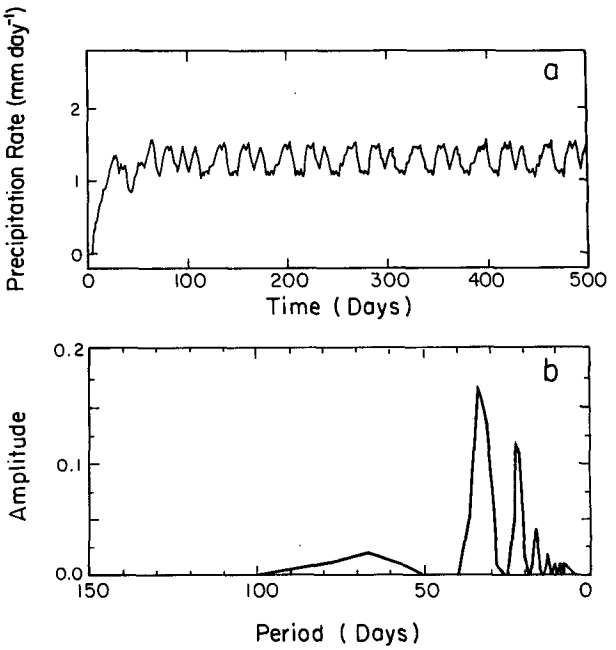

FIG. 2. (a) Simulated precipitation rate (mm day^{-1}) after application of an 11-day running mean, for a 500-day period in the control run. (b) The spectrum of the precipitation, analyzed from the precipitation data from day 300 to day 2000.

from day 1000 through day 1100. Here "perturbation" means the departure from the time average at each level. Approximately three oscillation cycles occur during the period shown. The perturbation values of the temperature, moisture, and radiative cooling rate each undergo a sign reversal in the vertical, near 850 mb. For example, in Fig. 3a, $T' > 0$ below 850 mb is accompanied by $T' < 0$ above 850 mb, and vice versa, indicating an oscillation of the lapse rate. Both positive and negative anomalies appear first at upper levels, and move down. A given anomaly reaches the lower levels about 10 days after it originates aloft. These fluctuations are quite similar to those reported by Hendon and Liebmann (1990; their Fig. 5). Moist convection occurs only below 650 mb, because the simple moist convective adjustment used to parameterize cumulus convection does not transport moisture above this level.

To analyze the mechanism of the oscillation, we focus on one cycle between days 52 and 90 (recall that the 100-day period shown in the figure begins 1000 days into the simulation), as shown in Fig. 3. Starting around day 52 a warming occurs below 850 mb, while radiative cooling is evident aloft. At the same time, there is a drying above 850 mb and a moistening below. The mixing ratio is apparently being controlled by the temperature, indicating saturation at the levels in question. Around day 60, both T' and q' reach maximum positive values below 850 mb, while cooling and drying continue above. Convection then intensifies, as measured by the precipitation rate.

At the lower levels, this more intense convection leads to cooling and drying; this is to be expected from moist convective adjustment. Above 850 mb, the mixing ratio begins to increase at about day 63, while cooling continues until day 68, when the precipitation rate becomes very intense. During the time when the temperature is decreasing but the mixing ratio is increasing, the air is obviously unsaturated.

The phase relations between T' and Q_R' after day 68 indicate that convection, which warms the upper levels, promotes the development of strong radiative cooling aloft. The stronger the radiative cooling becomes, the more it promotes convection by trying to steepen the lapse rate. The precipitation rate develops a secondary peak around day 82.

The transition from cooling to warming aloft during the period of intense convection indicates that intense convection controls the upper-level temperature, overpowering radiative cooling. The warming aloft stops around day 82, when cumulus convection weakens. This weakening of the convection seems to be due to drying at the low levels, in combination with the weakening lapse rate. In the absence of strong convective warming, radiative cooling regains control of the upper level temperatures, which begin to decrease.

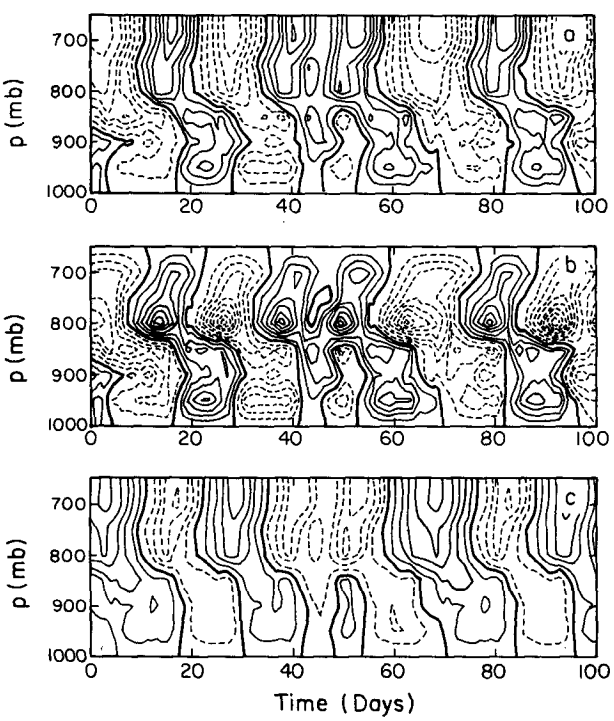

FIG. 3. (a) The perturbation temperature, T' (in K). (b) Perturbation mixing ratio, q' (in g kg^{-1}). (c) Perturbation radiative heating rate, Q_R' (in K day^{-1}), for the period from day 1000 through day 1100. Day 0 corresponds to day 1000 in the integration. The contour interval is 0.1 K for T', 0.1 g kg^{-1} for q', and 0.25 K day^{-1} for Q_R'. The contour lines in (c) are scaled by 200.

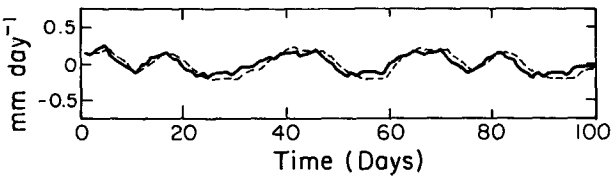

FIG. 4. Fluctuations of precipitation (solid line) and surface evaporation (dashed line), both in millimeters per day, as simulated with model 1.

The key feedbacks associated with the low-frequency oscillations may be summarized as follows. While the convection is weak, radiative cooling cools the air aloft, while moisture accumulates near the surface. This leads, eventually, to a high humidities and a steep lapse rate. This destabilization allows convection to intensify.

When convection intensifies, the surface evaporation rate increases;[1] a positive correlation between precipitation and evaporation is clearly seen in Fig. 4, which covers the same period of time as Fig. 3. The enhanced surface evaporation is due to near-surface drying produced by the convection.[2] Convective drying by itself would tend to shut off the convection, but the surface evaporation fights against this, allowing convection to continue longer than it otherwise would.

More intense convection leads to a warming aloft. Comparison of Figs. 3a and 4 shows that warming aloft occurs at the time of most rapid precipitation. The upper-level warming promotes and is opposed by stronger radiative cooling. Convective warming aloft by itself would tend to shut off the convection by stabilizing the lapse rate, but the radiative cooling fights against this, allowing convection to continue longer than it otherwise would.

Ultimately, the net result of more intense convection is that the upper levels become relatively warm and moist while the lower levels become dry. The low-level drying eventually leads to a weakening of the convection. Convection never actually stops; it only oscillates in intensity. More intense precipitation is associated with deeper convection.

The period of the oscillation is determined by several factors. One is the previously mentioned positive correlation between precipitation and the surface moisture flux. Without this effect, intense moist convection would quickly exhaust the available moisture, shutting itself off after a short time. An important factor favoring the relatively long period of the oscillation is the long time scale associated with radiative cooling. The

[1] Gray (1979) observed a positive correlation between precipitation and surface evaporation in tropical storms.

[2] In nature, convective "gustiness" may also tend to increase the evaporation rate during rainy periods.

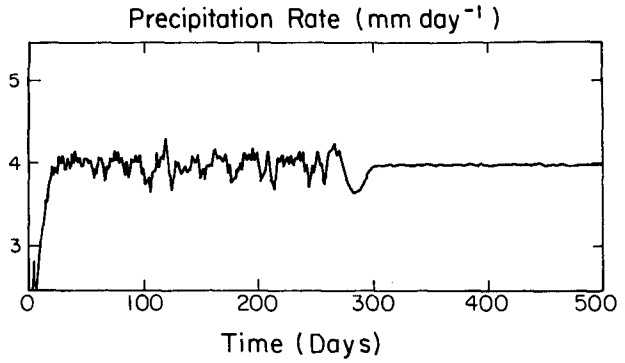

FIG. 5. Precipitation rate (mm day^{-1}) simulated with model 1 for days 1000–1500, in an experiment with a constant radiative cooling rate of 2.0 K day^{-1}.

vigor of the convection is partially determined by the rate at which radiation tends to destabilize the sounding. Weak radiative cooling allows relatively weak but prolonged convection.

Why does the model not produce a steady balance between radiative cooling and convective warming? As shown later, for some values of the parameters (e.g., lower sea surface temperatures) it does. The stationary equilibrium can become unstable, however, depending on the values of the external parameters.

We now present the results of some numerical experiments designed to clarify the nature of the oscillations.

2) EXPERIMENT WITH FIXED RADIATIVE COOLING

This experiment is designed to show that interactions between radiation and convection are crucial for the initiation and maintenance of the low-frequency oscillations. A constant radiative cooling rate of 2 K day^{-1} is used. The other conditions are the same as in the control run.

Figure 5 shows the precipitation rate obtained in this experiment. There are no fluctuations after the first 300 days; a steady balance is reached. A constant cooling rate allows no feedback between the radiative cooling and the convective warming. A steady state is reached when the warming due to convection and the surface sensible heat flux balances the prescribed constant cooling rate.

TABLE 2. Sensitivity of the model 1 results to surface wind speed (other parameters as in the control run).

$\lvert V_s \rvert$ (m s^{-1})	Major period (days)	Mean precipitation rate (mm day^{-1})	Amplitude (%)
2.0	45	1.4	32
10.0	28	1.1	9
15.0	12	0.9	9

TABLE 3. Sensitivity of the model 1 results to SST (other parameters as in the control run).

SST (°C)	Major period (days)	Mean precipitation rate (mm day^{-1})	Amplitude (%)
25	15	0.9	4
27	25	1.5	7
30	50	1.9	18
32.0	66	2.1	29

3) EXPERIMENT WITH A DRY ATMOSPHERE

With no moisture and no surface moisture flux, the solution is steady. This result is consistent with that obtained by Hayashi and Sumi (1986) in an "aqua planet" GCM simulation. When moist processes are omitted, the temperature profile relaxes to and stays at the pure radiative equilibrium profile, except near the surface where the sensible heat flux can balance radiative cooling.

4) SENSITIVITY TO SURFACE WIND SPEED, SEA SURFACE TEMPERATURE, AND RADIATIVE RELAXATION TIME

Table 2 shows how the oscillations are affected by variations of the surface wind speed. Throughout the range of wind speeds considered, oscillations occur. The period is longer and the amplitude is larger, however, when the surface wind speed is weaker. When the surface wind speed is 15 m s^{-1} the oscillation is very weak, with a period of only 12 days. With a high surface wind speed, the time scale for the accumulation of moisture in the mixed layer is short.

Table 3 shows how the precipitation oscillation varies with SST. A warmer SST favors a longer period and a larger amplitude. Figure 6 illustrates a cool SST case; there are no regular oscillations.

The results in Tables 2 and 3 and Fig. 6 are consistent with observations, which show that low-frequency oscillations of moist convection occur in regions of warm

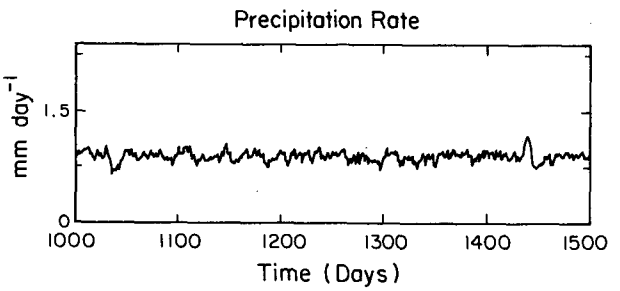

FIG. 6. Precipitation rate (mm day^{-1}) simulated with model 1 for days 1000–1500, in an experiment with a sea surface temperature of 298.15 K.

SST where the surface wind speed is relatively weak (Madden and Julian 1972).

Table 4 shows the effect of the radiation relaxation time, τ, on the oscillation. When τ is short, the radiative cooling is intense, so convection must be more active and hence the period of the oscillation becomes shorter for given SST and surface wind speed. On the other hand, since there is less time for moisture accumulation in the boundary layer, the amplitude of the oscillation is weak. An example is shown in Fig. 7; here τ = 10 days.

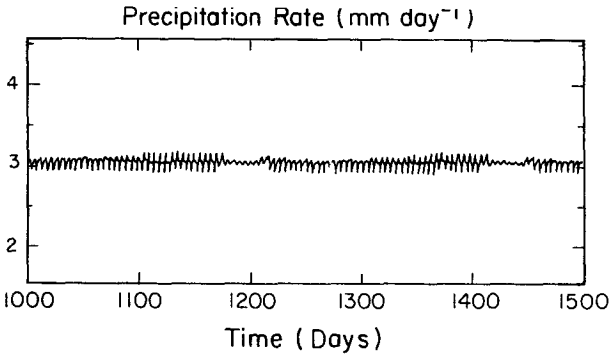

FIG. 7. Precipitation rate (mm day^{-1}) simulated with model 1 for days 1000–1500, in an experiment with a radiative relaxation time of 10 days.

3. A more complex model

The results obtained with model 1 illustrate that a low-frequency oscillating heat source can be initiated and maintained through interactions among radiation, moist convection, and the surface moisture flux. This supports our hypothesis. Because model 1 is highly idealized, however, the results obtained with it are easily questioned. This motivates us to repeat our experiments with a more sophisticated model.

a. Formulation

Model 2 is a nine-level one-dimensional model derived from the Colorado State University general circulation model (GCM), which has recently been described by Randall et al. (1989). As in model 1, the sea surface temperature and wind speed are fixed. The domain extends from the ocean surface to 50 mb. The physical processes included are essentially the same as those in model 1: radiation, convection, and the surface fluxes of sensible heat and moisture. The parameterizations themselves are radically different, however.

The boundary layer is represented by a variable-depth mixed layer. The depth of the boundary layer is regulated by turbulent entrainment and loss of mass into cumulus clouds. The effects of boundary-layer stratocumulus clouds are taken into account.

Cumulus convection that originates in the boundary layer is parameterized by the method of Arakawa and Schubert (1974); cumulus clouds that originate above the boundary layer are parameterized by moist convective adjustment. The Arakawa–Schubert parameterization takes into account the penetrative nature of deep moist convection. A conventional "large-scale precipitation" parameterization is also included.

The terrestrial and solar radiation parameterizations are those described by Harshvardhan et al. (1987, 1989). The diurnal cycle is included, as is the water vapor continuum. For purposes of the radiative transfer parameterizations, three types of clouds are allowed to form. They are cumulus anvils, supersaturation clouds, and boundary-layer stratocumulus clouds. Details are given by Randall et al. (1989).

The one-dimensional model is used for a variety of applications, including testing of new parameterizations and studies in which the effects of large-scale dynamics are either prescribed or neglected. An example is given by Randall et al. (1991).

In each of the various runs discussed below, model 2 was integrated for 1800 days with a time step of 30 minutes.

TABLE 4. Sensitivity of the model 1 results to τ (other parameters as in the control run).

τ (days)	Major period (days)	Mean precipitation rate (mm day^{-1})	Amplitude (%)
50.0	42	0.4	16
40.0	55	0.5	27
10.0	5	3.0	6

b. Results

1) A CONTROL RUN

We have made scores of simulations with model 2, beginning with some in which all physical parameterizations were included. The simulated perturbation precipitation rate from one such run is shown in Fig. 8a. Low-frequency oscillations are clearly evident. The spectrum (Fig. 8b) shows a peak at a period of about 50 days.

We then began systematically distilling the model down to its essentials, by turning off or simplifying various elements of the physical parameterizations. Tests showed that most of the details of the physical parameterizations were unnecessary for the oscillations, and that simplifying the model actually allowed the oscillations to emerge in somewhat simpler and cleaner form. Among the physical processes which proved to have no significant effect on the oscillations are the following: the diurnal cycle; variations of the boundary-layer depth; and the radiative effects of

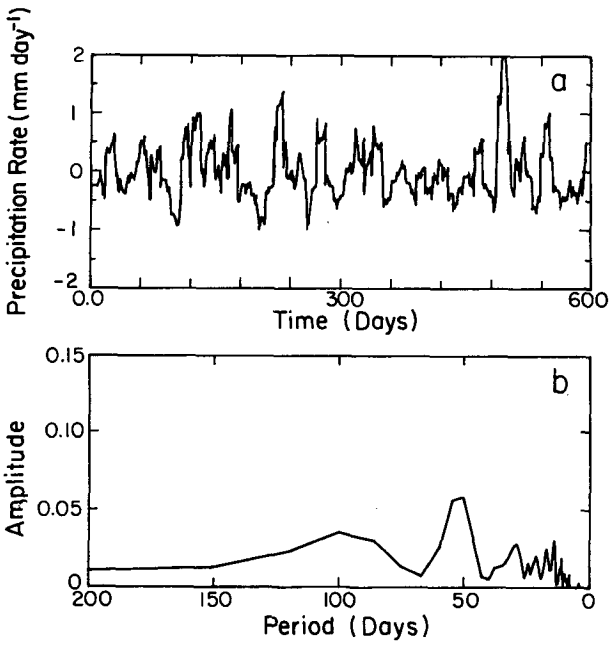

FIG. 8. (a) Simulated precipitation rate (in mm day^{-1}) from a 600-day segment of a run with a "complete" version of model 2. (b) Spectral analysis of the precipitation record shown in (a).

clouds. Of course, it is not surprising that these processes are not necessary for the oscillation, since none of them are included in model 1, which nevertheless oscillates.

In the "control run" discussed below, the diurnal cycle, variations of the boundary-layer depth, and the radiative effects of clouds have been turned off, for simplicity. The SST is 300 K, and the surface wind speed is 5 m s^{-1}.

The time variations of T' and q' are shown in Figs. 9a–b. These are for the last 600 days of the run. The cumulus precipitation rate for the same period is also shown in Fig. 9c (the same results were shown in Fig. 8a). The time-averaged precipitation rate is 1.29 mm day^{-1}, comparable to that obtained with model 1 (see Fig. 2). A 50-day oscillation is easily recognized, and stands out clearly under Fourier analysis (Fig. 9d). A vertical phase reversal of T' and q' is apparent in Figs. 9a and 9b, just as it was in Figs. 3a and 3b. Again, these fluctuations are similar to those reported by Hendon and Liebmann (1990). Since model 2 allows penetrative cumulus convection, the moisture variations extend through the whole atmospheric column. This is more realistic than the shallow moisture variations obtained with the moist convective adjustment scheme of model 1.

For the four times marked by letters A–D in Fig. 9c, low-level drying and upper-level moistening occur as the cumulus precipitation rate increases. While the convection is in its intense phase, the upper levels warm and moisten, and the lower levels dry. A minimum of

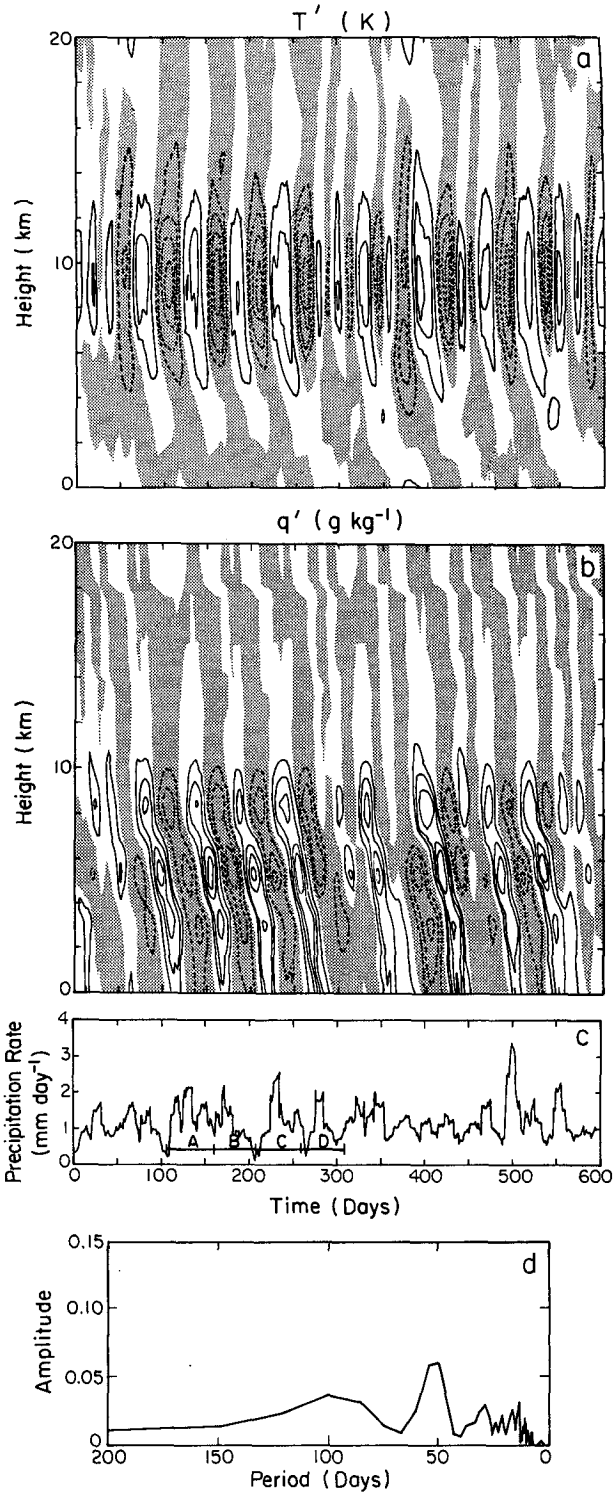

FIG. 9. (a) Temporal variations of perturbation temperature (K) for a 600-day period. Negative values are shaded, and zero contours are suppressed. The contour interval is 1 K. (b) As in (a) but for perturbation absolute humidity. The contour interval is 1 g kg^{-1}. (c) The time sequence of simulated precipitation rate (mm day^{-1}) for the same period. Times marked by A–D are discussed in the text. (d) The spectrum of the precipitation shown in (c).

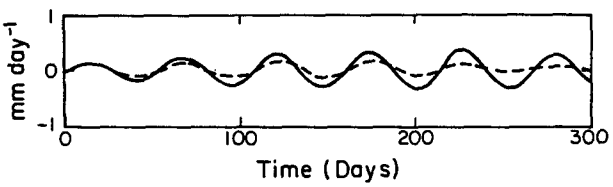

FIG. 10. Time sequence of bandpassed precipitation rate (solid line), and surface evaporation (dashed line), for a 300-day period.

Q_R' (i.e., strong cooling) in the upper levels occurs a few days after T' and q' have reached their maxima at the same levels. This phase relation among T', q', and Q_R' shows that the development of strong radiative cooling in the upper levels results from the warming (and moistening) there; it is, therefore, a consequence of cumulus convection. Following the intensification of the radiative cooling aloft, the cumulus precipitation rate increases.

The intense cumulus convection eventually dries out the mixed layer. Cumulus convection then weakens. As was the case with model 1, convection never actually stops. Weaker precipitation is associated with shallower convection. While the convection is suppressed, the low-level moisture is replenished, and at the same time radiative cooling steepens the lapse rate.

The period of intense convection is prolonged by a positive feedback between convection and surface evaporation. Figure 10 shows the bandpassed (Murakami 1987) time series of perturbation precipitation rate and the surface moisture flux for a 300-day period. The band center is at 50 days and its half-width is 8 days. The phase relationship between precipitation and evaporation shown in Fig. 10 is similar to that shown in Fig. 4, although in Fig. 10 the amplitude of P exceeds that of E, while in Fig. 4 they are comparable.

2) SENSITIVITY EXPERIMENTS

Experiments show that warmer SSTs favor longer periods and larger amplitudes. We also find, as with model 1, that low-frequency oscillations are favored by weak surface wind speeds.

In Table 5 we list some additional experiments and their results. Not surprisingly, elimination of interactions between solar radiation and other processes, by prescribing the time-averaged solar radiation from the control run, has no significant effect. When the infrared cooling rate is fixed in a similar way, however, the low-frequency oscillation disappears completely.

We have also found that with fixed surface fluxes of sensible and latent heat, model 2 produces irregular fluctuations with no clear spectral peak.

4. Concluding remarks

On the basis of our results, we conclude that the oscillations in models 1 and 2 result from essentially sim-

TABLE 5. Experiments and results from model 2.

	Experiment description	Result	Comments
No clouds in the radiative sense	All types of clouds are eliminated. SST = 300 K $\lvert V\rvert = 5$ m s^{-1}	30–50 day oscillations	Depth of significant variations in atmosphere is smaller than that in the control run.
Fixed SW radiation	Shortwave radiation transfer scheme is replaced by a fixed heating profile. Same SST and surface wind speed as in the control run.	Low-frequency oscillations	Results are similar to that in "cloud-free" run.
Fixed LW radiation	Longwave radiation transfer scheme is replaced by a fixed cooling profile. Standard SW scheme; clouds are not present. Same SST and $\lvert V\rvert$ as in control run.	No oscillations	Except for weak fluctuations in the PBL, no fluctuations are found in the model atmosphere.
Fixed surface fluxes	Surface sensible and latent heat fluxes are fixed. Other processes are the same as those in the "cloud-free" run.	Very slow variations	Irregular variations.
Fixed PBL depth	PBL depth is fixed at constant values. Other model processes are the same as in the cloud-free run. PBL Depth: 50 mb 100 mb 150 mb	Low-frequency oscillations	In the depth range examined the deeper the PBL is the more moisture is in the atmosphere and the larger the depth of the significant variation.

ilar interactions among radiation, cumulus convection, and the surface moisture flux. The similarity between the results of models 1 and 2 is amazing considering the numerous drastic differences in their physical parameterizations. Recently, Satoh and Hayashi (1992) have also reported spontaneous oscillations of both low and high frequency in a radiative–convective model.

The results from models 1 and 2 support the "forcing–response" hypothesis that the observed tropical low-frequency oscillations are forced by a localized oscillating heat source that does not depend on feedbacks from the large-scale motions to the convection. As shown by Salby and Garcia (1987) and Garcia and Salby (1987), a low-frequency tropical heat source excites waves that propagate slowly and have structures similar to the observed Madden–Julian waves. The forcing–response hypothesis originated with Yamagata and Hayashi (1984). They did not explain the nature of the oscillating heat source, however. Finding such an explanation has been the primary focus of our study.

Of course, we do not deny that the large-scale motions associated with the Madden–Julian oscillation can affect tropical convection. A wave will naturally tend to produce convection where it induces rising motion, and this dynamically induced convection will tend to propagate with the wave, at least to some extent. Our point is that such dynamically induced convection is not needed to explain the observed oscillations; it can be a side effect, not involved in any essential way.

Acknowledgments. At the time this collaboration began, Q. Hu was investigating the possibility that radiative–convective interactions could produce low-frequency oscillations. He was building a model that evolved into the "model 1" presented here. Independently, D. Randall found unexpected low-frequency oscillations in long runs with the one-dimensional version of the CSU GCM, which is essentially the "model 2" presented here. A hallway conversation led to the present study. A preliminary version of this work was presented by Hu (1992).

Professor Duane Stevens, now of the University of Hawaii, was Qi Hu's academic advisor during the early stages of this research, and also served as a member of his doctoral committee. We greatly appreciate the comments, suggestions and stimulating discussions offered by Professors Graeme Stephens and Wayne Schubert of Colorado State University, Dr. Klaus Weickmann of NOAA Environmental Research Laboratory, and Professor Chris Bretherton of University of Washington. Thanks are also due Professor Michael Ghil of UCLA for his encouragement and help. This research was sponsored by National Science Foundation Grant ATM-86-09731 through 1988 and early 1989, and has since been sponsored by NASA under Grant NAG-5-1058, and by the U.S. Department of Energy under Grant DE-FG02-89ER-69027.

Computing resources were provided by NCAR's Scientific Computing Division; NCAR is sponsored by the National Science Foundation.

REFERENCES

Anderson, J. R., and D. E. Stevens, 1987: The presence of linear wavelike modes in a zonally symmetric model of the tropical atmosphere. *J. Atmos. Sci.,* **44,** 2115–2127.

Arakawa, A., and W. H. Schubert, 1974: Interaction of a cumulus cloud ensemble with the large-scale environment: Part I. *J. Atmos. Sci.,* **31,** 674–701.

Chang, C. P., 1977: Viscous internal gravity waves and low-frequency oscillations in the tropics. *J. Atmos. Sci.,* **34,** 901–910.

——, and H. Lim, 1988: Kelvin wave–CISK: A possible mechanism for the 30–50 day oscillations. *J. Atmos. Sci.,* **45,** 1709–1720.

Emanuel, K. A., 1987: An air–sea interaction model of intraseasonal oscillations in the tropics. *J. Atmos. Sci.,* **44,** 2334–2340.

Garcia, R. R., and M. L. Salby, 1987: Transient response to localized episodic heating in the tropics. Part II. Far-field behavior. *J. Atmos. Sci.,* **44,** 499–530.

Gill, A. E., 1980: Some simple solutions for heat-induced tropical circulation. *Quart. J. Roy. Meteor. Soc.,* **106,** 447–462.

Gray, W. M., 1979: Hurricanes: Their formation, structure and likely role in the tropical circulation. *Meteorology over the Tropical Oceans,* D. B. Shaw, Ed., Royal Meteorology Society, 156–218.

Harshvardhan, R. Davies, D. A. Randall, and T. G. Corsetti, 1987: A fast radiation parameterization for atmospheric circulation models. *J. Geophys. Res.,* **92,** 1009–1016.

——, D. A. Randall, T. G. Corsetti, and D. A. Dazlich, 1989: Earth radiation budget and cloudiness simulations with a general circulation model. *J. Atmos. Sci.,* **46,** 1922–1942.

Hartmann, D. L., and J. R. Gross, 1988: Seasonal variability of the 40–50 day oscillation in wind and rainfall in the tropics. *J. Atmos. Sci.,* **45,** 2680–2702.

Hayashi, Y., 1970: A theory of large-scale equatorial waves generated by condensation heat and accelerating the zonal wind. *J. Meteor. Soc. Japan,* **48,** 140–160.

——, and A. Sumi, 1986: The 30–40 day oscillations simulated in an 'aqua-planet' model. *J. Meteor. Soc. Japan,* **64,** 451–467.

——, and S. Miyahara, 1987: A three-dimensional linear response model of the tropical intraseasonal oscillation. *J. Meteor. Soc. Japan,* **65,** 843–852.

Hendon, H. H., and B. Liebmann, 1990: The intraseasonal (30–50 day) oscillation of the Australian summer monsoon. *J. Atmos. Sci.,* **47,** 2909–2923.

Holton, J. R., 1972: Waves in the equatorial stratosphere generated by tropical heat sources. *J. Atmos. Sci.,* **29,** 368–375.

Hsu, H.-H., B. J. Hoskins, and F.-F. Jin, 1990: The 1985/86 intraseasonal oscillation and the role of the extratropics. *J. Atmos. Sci.,* **47,** 823–839.

Hu, Q., 1992: Low-frequency oscillations in radiative-convective models. Ph.D. thesis, Colorado State University, 196 pp.

Knutson, T. R., and K. N. Weickman, 1987: 30–60 day atmospheric oscillations: Composite life cycles of convection and circulation anomalies. *Mon. Wea. Rev.,* **115,** 1407–1436.

Krishnamurti, T. N., and D. Subrahmanyam, 1982: The 30–50 day mode at 850 mb during MONEX. *J. Atmos. Sci.,* **39,** 2088–2095.

Lau, K. M., and P. H. Chan, 1985: Aspects of the 40–50 day oscillation during northern winter as inferred from outgoing long wave radiation. *Mon. Wea. Rev.,* **113,** 1889–1909.

——, and L. Peng, 1987: Origin of the low-frequency (intraseasonal) oscillations in the tropical atmosphere. Part I: Basic theory. *J. Atmos. Sci.,* **44,** 950–972.

Lindzen, R. S., 1974: Wave–CISK in the tropics. *J. Atmos. Sci.,* **31,** 156–179.

Madden, R., and P. R. Julian, 1971: Detection of a 40–50 day oscillation in the zonal wind in the tropical Pacific. *J. Atmos. Sci.,* **28,** 1109–1123.

——, and ——, 1972: Description of global scale circulation cells in the tropics with a 40–50 day period. *J. Atmos. Sci.,* **29,** 1109–1123.

Manabe, S., and F. Möller, 1961: On the radiative equilibrium and heat balance of the atmosphere. *Mon. Wea. Rev.,* **89,** 503–532.

——, J. Smagorinsky, and R. F. Strickler, 1965: Simulated climatology of a general circulation model with a hydrologic cycle. *Mon. Wea. Rev.,* **93,** 769–798.

Murakami, T., 1987: Intraseasonal atmospheric teleconnection patterns during the Northern Hemisphere summer. *Mon. Wea. Rev.,* **115,** 2133–2154.

——, L. X. Chen, A. Xie, and M. L. Shrestha, 1986: Eastward propagation of 30–60 day perturbations as revealed from outgoing longwave radiation data. *J. Atmos. Sci.,* **43,** 961–971.

Neelin, J. D., I. M. Held, and K. H. Cook, 1987: Evaporation–wind feedback and low-frequency variability in the tropical atmosphere. *J. Atmos. Sci.,* **44,** 2241–2248.

Oort, A. H., 1983: *Global Atmospheric Circulation Statistics, 1958–73.* NOAA Prof. Paper No. 14.

Randall, D. A., Harshvardhan, D. A. Dazlich, and T. G. Corsetti, 1989: Interactions among radiation, convection, and large-scale dynamics in a general circulation model. *J. Atmos. Sci.,* **46,** 1943–1970.

——, ——, and ——, 1991: Diurnal variability of the hydrological cycle in a general circulation model. *J. Atmos. Sci.,* **48,** 40–62.

Rueda, V. O. M., 1991: Tropical–Extratropical Atmospheric Interactions. Ph.D. thesis, UCLA, 194 pp.

Salby, M. L., and R. R. Garcia, 1987: Transient response to localized episodic heating in the tropics. Part I: Excitation and short-time near-field behavior. *J. Atmos. Sci.,* **44,** 458–498.

Satoh, M., and Y.-Y. Hayashi, 1992: Simple cumulus models in one-dimensional radiative–convective equilibrium problems. *J. Atmos. Sci.,* **49,** 1202–1220.

Wang, B., 1988: Dynamics of tropical low-frequency waves: An analysis of the moist Kelvin wave. *J. Atmos. Sci.,* **45,** 2051–2064.

——, and J. Chen, 1989: On the zonal-scale selection and vertical structure of equatorial intraseasonal waves. *Quart. J. Roy. Meteor. Soc.,* **115,** 1301–1323.

Weickmann, K. M., and S. J. S. Khalsa, 1990: The shift of convection from the Indian Ocean to the western Pacific Ocean during a 30–60 day oscillation. *Mon. Wea. Rev.,* **118,** 964–978.

Yamagata, T., and Y. Hayashi, 1984: A simple diagnostic model for the 30–50 day oscillation in the tropics. *J. Meteor. Soc. Japan,* **62,** 709–717.

Yasunari, T., 1979: Cloudiness fluctuations associated with the Northern Hemisphere summer monsoon. *J. Meteor. Soc. Japan,* **57,** 227–242.

Zhu, B., and B. Wang, 1993: The 30–60-day convection seesaw between the tropical Indian and Western Pacific Oceans. *J. Atmos. Sci.,* **50,** 184–199.